3D Modelling of Laser Hardening and Tempering of

Hypo-eutectoid Steels

Giovanni TANI*, Leonardo ORAZI**, Alessandro FORTUNATO*, Giampaolo CAMPANA* and Alessandro ASCARI*

DIEM Department of Mechanical Construction Engineering, University of Bologna, Viale Risorgimento, 2 40136, Bologna, Italy.
E-mail: giovanni.tani2@unibo.it
** *DISMI Department of Science and Method for Engineering, University of Modena-Reggio Emilia, Via Amendola, 2 42100, Reggio Emilia, Italy*

In this paper a mathematical model solved by means of the finite differences method (FDM) for laser surface hardening of complex geometries is presented. The 3-D transient model characterizes a software package named Laser Hardening Simulator (LHS), which makes it possible to predict the extension of the treated area into the mechanical components and thus the hardened depth into the bulk material. The obtained microstructures and the resulting hardness with respect to the laser parameters and to the laser beam path strategy can be determined by considering the quenching and the tempering effects due to the overlapping trajectories. The initial workpiece microstructure is taken into account in the simulation by a digitized photomicrograph of the ferrite-pearlite distribution before the thermal cycle. In order to show the accuracy of the model, experimental trials were conducted on the keyway for spline machined on a hub made of SAE 1043. The domain discretization for the solution of the heat flux problem into the workpiece and for the diffusion of the carbon is carried out by means of a mesh generator strategy implemented into the code.

Keywords: Laser Hardening, Process Simulation, FDM, Carbon Steel

1. Introduction

The needs of modern industry to facing high production rates of many different products promoted a radical change in process setup and planning procedures. According to this, a transition occurred from the traditional trial-and-error routine, which caused a considerable waste of time and resources, to a modern approach based on process simulation. This change was possible thanks to the possibility to exploit the power of modern calculators on accurate and customized modelling algorithms.

In particular heat based manufacturing technologies such as welding, cutting, and heat treatment should take great advantages, in terms of process optimization and setup, from these new capabilities. Besides, the possibility of implementing the above mentioned processes directly on the production line, through the exploitation of anthropomorphic robots, made possible to avoid the involvement of third party suppliers in production. According to this, process simulation gets even more interest as a mean of optimization and time saving especially when highly differentiated product batches have to be manufactured. A clear example of this situation is the possibility of integrating a LASER surface heat treatment facility on the production line instead of exploiting an off-line induction or flame one.

Many researchers stressed on the simulation of this process starting from Ashby et al. [1], who exploited a monodimensional analytic model, and developed towards more complex numerical solutions proposed by Shin et al. [2], Rappaz et al. [3] and Ohmura et al. [4]. Any of these approaches implies the exploitation of two different models: one for temperature field determination and the other for carbon diffusion evaluation.

In particular, in the present work great efforts have been made in order to advance the discussed models. By starting from a simplified analytical diffusion model as presented in [1], a new numerical approach was developed which is able to predict not only the austenite-martensite transformation as in [1], [2], [3] and [4] but also the tempering effects on the pre-treated area [5] and the intermediate microstructures such as residual austenite, bainite and pearlite as modelled in [6] [7]. The latter facility can be particularly important when workpieces with small dimensions have to be heat treated because the effect of the multi-pass trajectories causes a reduction of the cooling velocity. In fact, in the previous models the error in hardness prediction increases with the distance from the upper surface due to the fact that intermediate microstructures were not considered while the actual cooling velocity decreases and microstructures like bainite can transform.

This work deals with a comprehensive model which includes the capability of predicting any metallurgical microstructures occurring after the heat treatment.

The possibility of implementing the laser beam path through a standard CN ISO format has also been taken into consideration.

An advanced 3D mesh generator was adopted in order to allow the simulation of the process applied on complex shapes.

Further efforts have been made towards the possibility of predicting the tempering effect due to overlapping beam trajectories.

2. Laser Hardening Model

The complete description of the adopted differential equations for temperature field calculation, together with the used algorithms and their stability criterions, were already presented by the authors in [5]. The time dependent temperature distribution is determined by the solution of the Fourier equations as expressed in equation 1.

$$c_p \rho \frac{\partial T}{\partial t} = \frac{\partial}{\partial x}\left(k\frac{\partial T}{dx}\right) + \frac{\partial}{\partial y}\left(k\frac{\partial T}{\partial y}\right) + \frac{\partial}{\partial z}\left(k\frac{\partial T}{\partial z}\right) + q \qquad (1)$$

Where:
c_p specific heat [J/kgK]
ρ material density [kg/m^3]
k target thermal conductivity in [W/mK]
q laser heat flux into the material in [W/m^3]

Laser surface hardening happens without melting or vaporization of the target surface and the laser-material interaction is limited to the evaluation of the heat flux into the bulk due to heat conduction from the surface.

When the eutectoid temperature is reached into the bulk material pearlite dissolution and austenite homogenization begin. The kinetics of this transformations are governed, respectively, by the dissolution law as in [1] for the pearlite transformation into the austenite phase and by the second Fick's equation, here presented as equation 2:

$$\frac{\partial C_v}{\partial t} = \frac{\partial}{\partial x}\left(D_v\frac{\partial C_v}{dx}\right) + \frac{\partial}{\partial y}\left(D_v\frac{\partial C_v}{\partial y}\right) + \frac{\partial}{\partial z}\left(D_v\frac{\partial C_v}{\partial z}\right) \quad (2)$$

Where:
C_v solute concentration in the v phase
D_v the solute diffusivity in the v phase

Equations 1 and 2 were solved by creating two independent mesh grids. The sizes of the grids took into account the stability criterion of the two algorithms adopted for the solution of the equations and they were chosen in order to minimize the calculation time without losing in accuracy [5].

In particular, the Finite Difference Method (FDM) technique was used in order to solve equation 1 and the algorithm was customized in order to take into account a variable grid [9].

The initial microstructure of the material is assessed by digitalized photomicrographs. The authors developed an automatic procedure which is able to directly convert the microstructures data stored by the photomicrograph into a text matrix [8]. Every character of that matrix is a meshing cell which is marked as either ferrite, or pearlite or transition between those phases.

The microstructures resulting from the quenching were predicted by implementing the models in [6] and [7]. These models allow to extend the hardening prediction to workpieces with small dimensions when the effect of the multipass trajectories cause a reduction of the cooling velocity and, in generale, to any surface hardening process where not the whole austenite is transformed to martensite [1].

The complete software package is named Laser Hardening Simulator (LHS).

2.1 Model validation

LHS implements a routine for generating the discretization of the domain. As example a keyway for spline machined on the central hub of a roller torque limiter is meshed, see figure 1. For the rake of simplicity, by setting proper boundary conditions, only half geometry can be modeled.
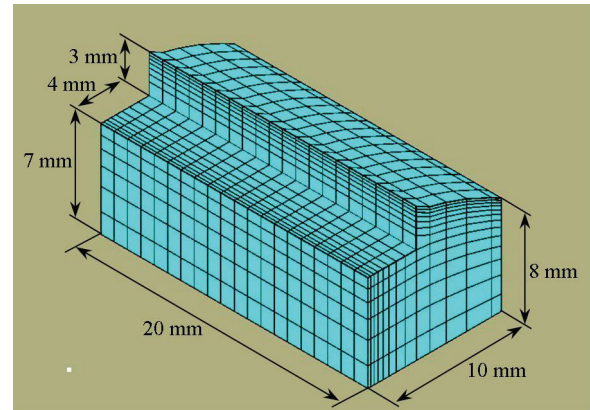

Fig. 1 Keyway meshing.

Thanks to this a finer grid was adopted in the zones nearest to the surface, in which the temperature gradient is high, while in the inner zones a coarse grid was exploited (see figure 1). This solution made possible to achieve a good compromise between accuracy of results and computation time.

The possibility to acquire the finite elements coordinates from commercial meshing utilities was also implemented in order to make the LHS software more attractive and user-friendly for the industrial environment.

The simulation was conducted considering a laser beam moving on a straight line parallel to the axis of the keyway and with 2 mm distance from its edge, as shown in figure 5.

Considering the case study represented in figure 1, the technological requirement of the producer of the sample hub is the hardening of the lateral surface of the keyway, in particular a 1 mm deep hardened layer with at least 550

Table 1 Laser parameters adopted for the simulation

Laser spot diameter	Laser velocity	Laser power
7 mm	0.4 m/min	1200 W

HV$_{1000}$ is required.

The aim of the simulation is to predict the hardened depth according to laser parameters presented in table 1.

The workpiece material is a normalized SAE 1043 steel with the initial microstructure showed in figure 2.
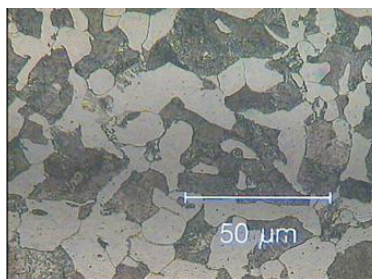
Fig. 2   Initial microstructure: ferrite-pearlite distribution.

The white zones in figure 2 are the ferrite grains while the darker ones represent the pearlite colonies. A further increase in the magnification of the picture could permit to appreciate the mean step of the lamellar pearlite that is about 2 μm.

2.2   The prediction of tempering effects

The tempering of the martensite microstructures occurs when the trajectories of the laser beam cause the re-heating of the transformed area. The path strategy of the beam is a critical factor for the success of the process: overlapping trajectories must be avoided and, in general, the sequences of the paths must allow the maximum cooling velocity of the treated area.
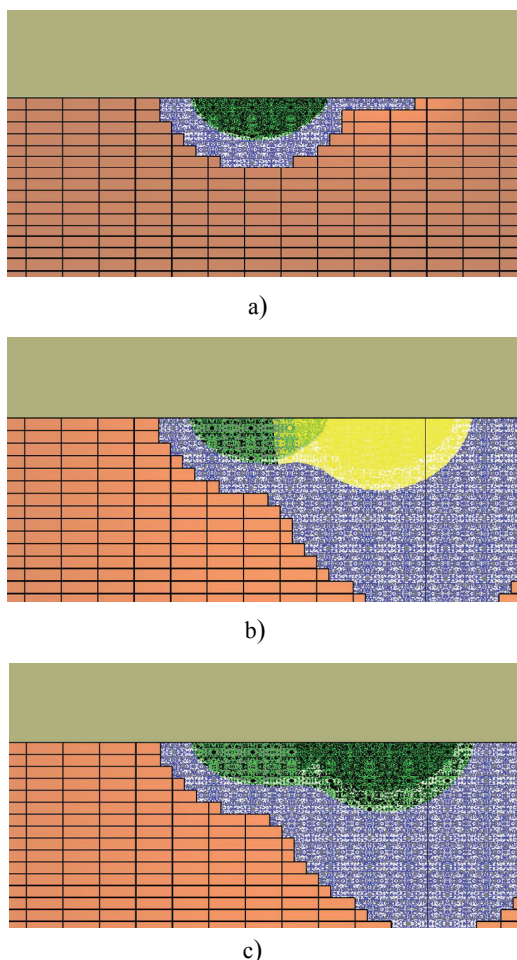

a)

b)

c)

Fig. 3   Tempering effects on the martensite microstructure

As an example, in figure 3 a temporal sequence of the surface hardening is presented. The simulation concerns a transversal view of a laser hardening obtained with a straight-lined trajectory of the laser beam. The spot diameter was set to 7 mm, and a TEM_{00} energy distribution was exploited. The distance between the first and second trajectory was set equal to the beam diameter. According to figure 3a and 3b the hardened area is represented with the green/black color, while the austenite is in yellow. The second laser path causes a re-austenitization of the martensite and, after the quenching, the hardness of the first treated area is lower. This effect is pointed out by the light green/black color in figure 3c. At the same time, the second treated area is bigger due to the fact that during the second laser path the workpiece is already heated. At this stage of the code development, the tempering effects are predicted only considering the decreasing of the pre-treated areas and the decreasing of the related hardness due to the resulting microstructures after subsequent quenching. In future works a detailed modelling of the overheating of the re-austenitization will be proposed together with a model for the calculus of the hardness of the structures only tempered and not re-austenitized.

3.   Experimental

The experimental part of this work was performed on a hub belonging to a roller torque limiter. The induction surface hardening of the four keyways for spline machined on its external surface (see Figure 4) is nowadays performed by a third party supplier. According to this the possibility of substituting the traditional off-line induction process with a modern LASER on-line one is worth to be investigated and could be an interesting solution for the manufacturer of the mentioned component.
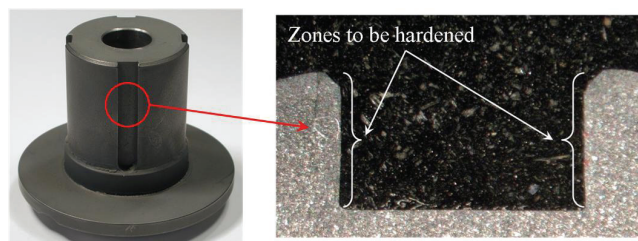

Fig. 4   Sample of the component to be treated and zones of interest

The manufacturer of the component requires a hardness of at least 550 HV_{1000} on a layer with a minimum depth of 1 mm. The zones which must be actually hardened are limited to both the vertical walls of the keyways as shown in figure 4.
The equipment used in this phase was a FAF 3 kW CO2 laser source and the process parameters exploited are summarized in table 1. The position of the laser beam with respect to the zone to be treated is described in figure 5.

As shown in figure 4 the hub was previously coated with a thin layer of spray graphite with the aim to increase the absorptivity of the working surface.

The resulting treated zone is shown in figure 6, where the black line marks the direction of hardness measurement.
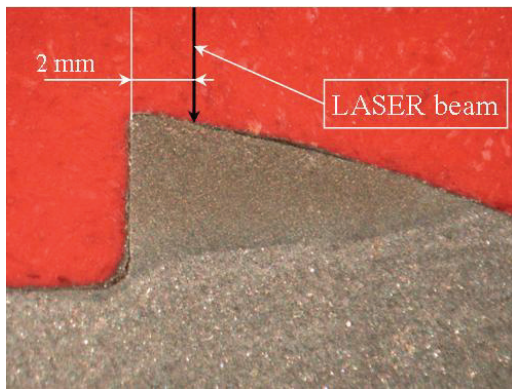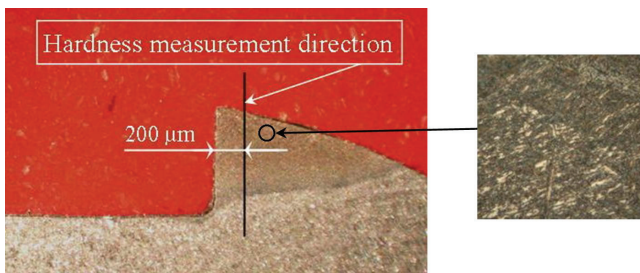
Fig. 5 Laser beam position

Fig. 6 The LASER treated specimen and a 1000x magnification of the martensitic zone

4. Results and Discussion

The process described in the previous paragraph was simulated using the software LHS. The simulations were conducted using the same parameters of the experiment and the main results are showed in figures 7. During the simulation, the laser beam axis is placed 2 mm away from the edge as in figure 5.
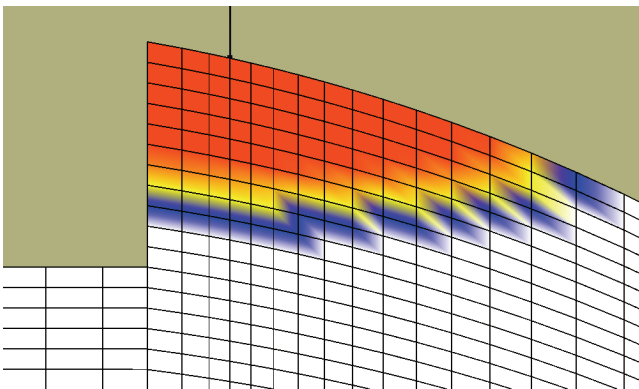

Fig. 7 Simulation frame after 1.2 sec: the hardening prediction during quenching

Figure 7 represents the simulation of the quenched phase after 1.20 s. The martensitic structures, indicated with the red color, has different intensity in the treated zone. It has lower intensity in correspondence of the zone were the martensite transformation is not uniform, the bottom zone, and higher intensity at the bottom where the austenitization was completed. The yellow color represents the hardness of the intermediate structures obtained after

quenching and they separate the martensite from the pearlite and ferrite phases which have only reached the eutectic temperature without being involved in the hardening process. As a consequence, the hardness decreases and it reaches the lowest value where no structural transformation happens: the pearlite/ferrite overheating indicated by the blue color.

The grid dimension, adopted and represented in figure 7, is 250 μm in the depth direction so that the hardness resulting form the complete martensite formation is predicted as presented in figure 8.
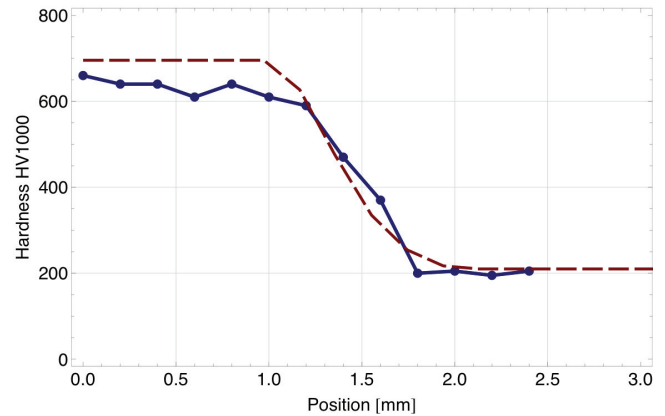

Fig. 8 Hardness comparison

Figure 8 represents the comparison between the predicted and the experimental hardness. The measurement were carried out 200 μm from the edge of the keyways, as showed in figure 6, by means of Vickers test with 1 kg pre-load. The measurements, performed every 200 μm, proved that the treated depth is bigger than 1 mm as required. After about 1 mm, as predicted in figure 7, the hardness decreases until 1.5 mm where the hardness of the base material is reached. As proved in figure 8 and predicted by LHS a transition of about 500 μm occurs.

In this case the accuracy of the code is high in terms of the prediction of the extension on the treated area and in terns of predicted hardness.

In particular, by predicting the fraction of bainite and pearlite transforming during quenching the transition between the maximum hardness and the base hardness can be modeled.

As a conclusion, the overall results of the simulation are consistent with the experimental ones.

5. Conclusion

A 3-D transient mathematical model of the laser surface hardening for hypo-eutecoid steel is presented. The software package, LHS, predicts the treated area and the related hardness according to the laser parameters and to the laser beam path strategy.

A generalized model for the prediction of the microstructures after quenching is considered which is suitable for every heat treatment.

LHS also implements a routine which generates the grid of the domain or allows to import a meshed domain from any commercial code.

References

[1] M. F. Ashby, K. E. Easterling: Acta Metall. 32 (1984) 11. (Journals)
[2] S. Skvarenina, Y. C. Shin: Surface and Coating Technology 201 (2006) 6. (Journals)
[3] A. Jacot, M. Rappaz, R. C. Reed: Acta Mater. 46 (1998) 11. (Journals)
[4] E. Ohmura, K. Inoue, K. Haruta: JSME International Journal 32 (1989) 1, 45-53. (Journals)
[5] G. Tani, L.Orazi, A. Fortunato, G. Campana, G. Cuccolini: Proc of Spie, Photonics (2007). (Conference Proceedings)
[6] S. Denis, D. Farias and A. Simon: ISIJ International. 32 (1992) 3. (Journals)
[7] T. Reti, Z. Fried, I. Felde: Computational Material Science 22 (2002) 261-278. (Journals)
[8] G. Tani, A. Ascari, L. Orazi: Proc. of ASME, International Manufacturing Science and Engineering Conference MSEC (2007). (Conference Proceedings)
[9] J. Peiro, S. Sherwin,: Finite Difference, Finite Element and Finite Volume Methods for Partial Differential Equation, Handbook of Material Modeling. Vol 1, 2th edition, 2005. (Books)